frontiers | Frontiers in Drug Discovery

TYPE Original Research
PUBLISHED 17 September 2025
DOI 10.3389/fddsv.2025.1673051



OPEN ACCESS

EDITED BY
Danilo Ciccone Miguel,
State University of Campinas, Brazil

REVIEWED BY
Krishnan Rangan,
Birla Institute of Technology and Science, India
Sérgio Veloso,
University of Vigo, Spain

*CORRESPONDENCE
Sara La Manna,
sara.lamanna@unina.it

RECEIVED 25 July 2025
ACCEPTED 05 September 2025
PUBLISHED 17 September 2025

CITATION
Pota G, Florio D, Cimmino L, Netti PA, Panzetta V, Marasco D and La Manna S (2025) Influence of divalent metal ions on gelation of a short heterochiral peptide.
*Front. Drug Discov.* 5:1673051.
doi: 10.3389/fddsv.2025.1673051



# Influence of divalent metal ions on gelation of a short heterochiral peptide

Giulio Pota[1,2], Daniele Florio[3], Luca Cimmino[3], Paolo Antonio Netti[4,5], Valeria Panzetta[4,5], Daniela Marasco[1,2] and Sara La Manna[1,2]*

[1]Department of Pharmacy, University of Naples Federico II, Naples, Italy, [2]Interuniversity Research Center on Bioactive Peptides (CIRPEB) "Carlo Pedone", Naples, Italy, [3]IRCCS SYNLAB SDN, Naples, Italy, [4]Department of Chemical, Materials and Production Engineering, University of Naples Federico II, Naples, Italy, [5]Interdisciplinary Research Centre on Biomaterials (CRIB), University of Naples Federico II, Italian Institute of Technology, Naples, Italy

Peptide self-assembly has emerged as a powerful and versatile strategy for the design of supramolecular biomaterials with tunable structural and functional properties. Through the precise organization of short peptide sequences, it is possible to construct nanostructured materials that mimic biological architecture and respond to specific environmental cues. Among the various design elements that influence peptide assembly, the incorporation of metal ions has gained increasing attention as a means to modulate material properties and endow biofunctionality. In this study, we investigated the distinct effects of four divalent metal cations—calcium ($Ca^{2+}$), magnesium ($Mg^{2+}$), zinc ($Zn^{2+}$), and copper ($Cu^{2+}$)—on the hydrogel-forming capabilities of Ac-(L-Phe)-(L-Ile)-(L-Asn)-(D-Tyr)-(L-Val)-(L-Lys)-$CONH_2$ (FINyVK), an ultrashort heterochiral hexapeptide derived from the second helix of the C-terminal domain of Nucleophosmin 1 (NPM1), a nucleolar protein implicated in both structural maintenance and disease-related aggregation. This peptide sequence is amyloidogenic and capable of forming hydrogels under appropriate conditions. By employing a comprehensive set of biophysical techniques, including circular dichroism (CD), rheology, electron microscopy, and thermal analysis, we characterized the conformational and morphological properties of hydrogels formed both in the presence and absence of metal ions. Our findings revealed that metal coordination can significantly alter peptide assembly pathways, influencing key features such as fibrillar thickness, network porosity, and the kinetics of gelation. Notably, different cations impart distinct effects: while alkaline earth metals like $Ca^{2+}$ and $Mg^{2+}$ enhance fibrillar alignment and promote reversible gelation, transition metals such as $Zn^{2+}$ and $Cu^{2+}$ tend to disrupt ordered structures due to stronger coordination with aromatic residues. These results underscore the utility of metal–peptide interactions as a rational design principle for engineering advanced peptide-based hydrogels.

KEYWORDS

**divalent cations, peptide self-assembly, hydrogels, rheology, heterochirality**

## Introduction

Over the past 2 decades, peptide self-assembly has emerged as a powerful and versatile approach for developing supramolecular smart materials (Levin et al., 2020; Chang et al., 2024; Mu et al., 2024). This process, which involves the spontaneous organization of individual molecules into ordered structures, plays a central role in both natural biological systems (Kuila and Nanda, 2024), and synthetic biomaterials like nanoparticles, fibrils, nanotubes, and vesicles or hydrogels (Zhou et al., 2023; Hua and Shen, 2024; Sahu and Chakraborty, 2024).

Peptides, in particular, are highly attractive molecules for their chemical versatility, ease of synthesis (Marasco et al., 2008), biodegradability, and intrinsic ability to encode biological functions (De Soricellis et al., 2023). Self-assembled peptide-based systems have gained significant attention for a wide range of biomedical applications, including drug delivery, tissue engineering, vaccine formulation, and biosensing (De Soricellis et al., 2023). In these contexts, their performance depends not only on the mechanical properties of the resulting hydrogels but also on the precise molecular organization at the nanoscale (Fichman and Gazit, 2014; La Manna et al., 2021).

Short or ultra-short sequences composed of 2–7 amino acids are especially appealing due to their structural simplicity and high reproducibility (Gupta et al., 2020). Aromatic moieties exert crucial functions in self-recognition mechanism: stacking interactions rather than mere hydrophobicity provide energetic contribution as well as order and directionality in supramolecular structures (Huang et al., 2025). In addition, the incorporation of D-amino acids is a facile approach to modulate the physicochemical and biological properties of peptide-based hydrogels (Melchionna et al., 2016). At molecular level, a proposed model suggests that a kink at the interface between L- and D-blocks leads to the assembly of flat monolayers with different faces bearing both hydrophobic and charged interactions (Clover et al., 2020).

To optimize hydrogel performance, it is possible to act not only on the peptide sequence, through the rational selection of amino acids and stereochemistry, as previously described, but also by introducing exogenous components such as divalent metal ions ($M^{2+}$) (Shen et al., 2022).

Self-assembling peptides can interact strongly with $M^{2+}$ ions, which in turn can modulate their secondary structure, self-assembly dynamics, and functional properties. Metal coordination introduces additional noncovalent interactions that can drive peptide self-assembly, often resulting in the formation of supramolecular metallogels, where metal ions play key structural roles by coordinating with amino acid or peptide-based gelators (Pal and Roy, 2022). $M^{2+}$ ions can bind to various functional groups—including amino, carboxyl, and hydroxyl moieties—on peptide chains, significantly influencing the mechanical, structural, and biological properties of the resulting hydrogels (Shao et al., 2024).

Under physiological conditions, $M^{2+}$ ions are often gradually released from hydrogels, and depending on the specific cations employed, they can serve various biological functions. For example, Qian et al. developed a hyaluronic acid (HA)-Cu hydrogel by coordinating hydrazide-modified HA with $Cu^{2+}$ ions, resulting in a material with good biocompatibility and notable antibacterial activity against *Escherichia coli* and *Staphylococcus aureus* (Qian et al., 2022). Similarly, the incorporation of $Mg^{2+}$ into hydrogels has been shown to enhance the adhesion of bone marrow stromal cells by promoting the expression of fibronectin and integrins at cell adhesion sites. A hydrogel system combining $Mg^{2+}$ and curcumin was reported to support rotator cuff tendon-to-bone healing through anti-inflammatory and pro-differentiation mechanisms (Chen et al., 2021). $Ca^{2+}$ and $Mg^{2+}$ have also been reported to promote cell migration and tissue regeneration; in one study, a $Ca^{2+}$/$Mg^{2+}$-releasing hydrogel facilitated the infiltration of endogenous cells and enhanced new bone formation (Yu et al., 2023). On the other hand, the strong chelating capacity of $Zn^{2+}$ could be used to direct the formation of supra-molecular dodecapeptide-based hydrogels to be used as carrier systems for hydrophobic cargoes (Wu et al., 2024). Furthermore, versatile bio-inspired self-healing hydrogels were produced by non-covalent crosslinking induced by $Zn^{2+}$-His coordination (Tunn et al., 2019).

When selecting an appropriate amyloid sequence, it is important to recognize that proteins often contain short sequence fragments which, although sometimes buried within their three-dimensional structures, exhibit unexpected properties. These fragments can be harnessed to design innovative peptide-based molecules with unique characteristics (Seidi et al., 2021; La Manna et al., 2022b; Gao et al., 2024).

In recent years, we have reported the hydrogel-forming ability of an amyloidogenic hexapeptide fragment (residues 268–273, FINYVK) derived from Nucleophosmin 1 (NPM1) (Florio et al., 2021). This fragment is located within the second helix of the three-helix bundle that forms the C-terminal domain (CTD) of NPM1 (Russo et al., 2017), a homopentameric nucleolar protein essential for chaperone activity and the maintenance of nucleolar organization through liquid–liquid phase separation (LLPS) (Mitrea et al., 2018). Notably, NPM1 is the most frequently mutated gene in a subtype of Acute Myeloid Leukemia (AML), with mutations occurring within the third helix of the CTD that promote amyloid-like self-aggregation and the formation of cytotoxic fibrils (La Manna et al., 2022a; Marasco et al., 2024). To further explore the chemical diversity of novel self-assembling sequences, we previously introduced single D-amino acid substitutions and analyzed the gelation properties of the resulting hexapeptides. Using various biophysical techniques, we found that the modified sequences were capable of forming hydrogels with good biocompatibility, though they exhibited different conformational intermediates during aggregation. Among them, the peptide derived from the substitution of $Tyr^{271}$ with its D-enantiomer (FINyVK) stood out for its unique features: prolonged β-sheet stability lasting up to 65 h, the highest critical aggregation concentration (CAC), and the greatest cytocompatibility among the tested sequences (Florio et al., 2021). A schematic representation of the design strategy that led to the development of the heterochiral, bioinspired peptide FINyVK is shown in Figure 1.

In this study, we investigated the effects of divalent metal ions in promoting the hydrogelation of the FINyVK peptide, with the aim of developing unexplored novel materials. Specifically, we selected two alkaline earth metals ($Ca^{2+}$ and $Mg^{2+}$) and two transition metals ($Zn^{2+}$ and $Cu^{2+}$) based on their reported ability to modulate both the structural and functional properties of biomaterials. These metal

10.3389/fddsv.2025.1673051

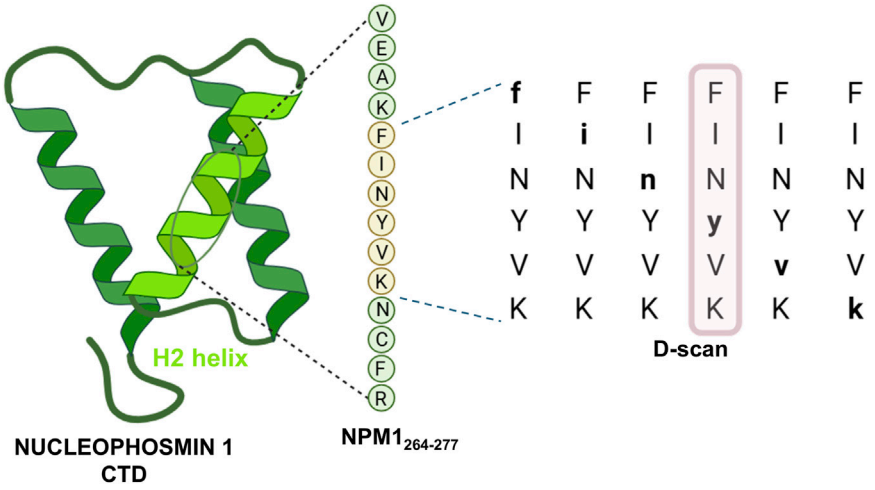


FIGURE 1
Graphical insight into the determination of FINyVK as relevant self-assembling monomeric unit.

ions are known not only to enhance the stability of supramolecular assemblies, but also to influence a broad range of biological responses. By choosing these cations, we sought to explore how metal–peptide interactions can be harnessed to fine-tune the self-assembly process and tailor the properties of the resulting hydrogels in a biologically relevant context.

# Materials and methods

## Materials

Amino acids for peptide synthesis were obtained from Iris Biotech (Marktredwitz, Germany), while solvents used for synthesis and HPLC analyses were purchased from Romil (Dublin, Ireland). Chloride salts of bivalent cations ($CaCl_2$, $ZnCl_2$, $MgCl_2$, $CuCl_2$), hexafluoro-2-propanol (HFIP), monobasic sodium monophosphate (ReagentPlus®, ≥98.5%), sodium phosphate dibasic (ACS reagent, ≥98.5%), boric acid (ACS reagent, ≥99.5%), sodium tetraborate decahydrate (Borax, ACS reagent ≥99.5%) where purchased from Sigma Aldrich (Merck, Milan, Italy).

## Peptide synthesis

Bioinspired heterochiral peptide Ac-FINyVK-$CONH_2$ (pI = 10.38, $M_w$ = 823.98 g/mol) was synthesized and purified as described before (Florio et al., 2021). Peptide before each experiment underwent to a monomerization treatment, performed dissolving the purified peptide in HFIP/$H_2O$ = 1/1 v/v for 4 h, removing the HFIP by $N_2$ flux and freeze drying the resulting peptide.

## Hydrogel preparation

Neat hydrogels were produced following the revised protocol described by Chen et al. (2022). Different amounts of peptide were dissolved in borate buffer (20 mM, pH 8.5), sonicated for 15 min and vortexed for 45 s. The occurrence of gelling was assessed by inverted tube test every 15 min. Cations-hydrogels were obtained the same way by adding chloride salts ($MgCl_2$, $CaCl_2$, $ZnCl_2$, $CuCl_2$) at 1:1 M ratio with the peptide.

## Scanning electron microscopy (SEM)

The morphology of peptide hydrogels, in the presence and absence of divalent cations, was analyzed using field-emission SEM (Phenom_XL, Alfatest, Milan, Italy). Specifically, ~30 µL of a gel was drop-cast on an aluminium stub and drying under vacuum to prepare the samples. For 75 s, a thin layer of gold was sputtered at a current of 25 mA. Following the introduction of the sputter-coated samples into the specimen chamber, micrographs were taken using a secondary electron detector (SED) at an accelerating voltage of 15 kV. The ChemiSEM Technology (Alfatest) enables EDS analysis in the presence of divalent cations performed in live mode.

## Circular dichroism (CD)

CD measurements were performed on both monomeric and hydrogel forms of peptide with divalent cations at 1:1 ratio. In the first case, 400 µM peptide was dissolved in borate buffer 10 mM pH 8.5, submitted to wavelength scan in the wavelength range 190–260 nm, at 25 °C using a Jasco J-1500 spectropolarimeter (JASCO, Tokyo, Japan), employing a 0.1 cm path-length quartz cuvette. Thermal stress experiments were carried out on pre-formed hydrogels, at 1 mM concentration in borate buffer 10 mM. Specifically, the variation of CD signal upon temperature increase was analysed by heating the samples from 20 °C to 90 °C, with a heating rate of 1 °C/min and monitoring the CD signal at the wavelength of the minimum of all samples, registered at 20 °C. Full-scan spectra of the hydrogels were also acquired every 10 °C.

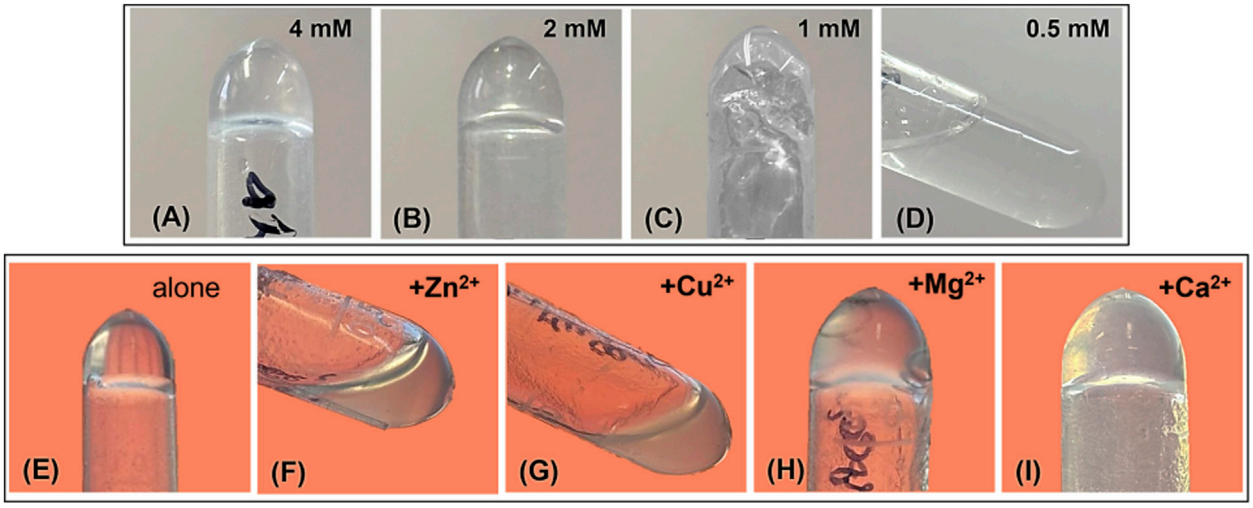


FIGURE 2
Analysis of gel formation by tube inversion method **(A–D)** at different peptide concentrations and **(E–I)** in the presence of divalent cations at 1:1 M ratio with peptide at 2.0 mM.

## Rheological tests

Rheological measurements on hydrogels were carried out using a stress-controlled shear rheometer (Anton Paar MCR 502) equipped with a 25 mm parallel plate geometry and a Peltier temperature control system. For the gelation test, 0.8 mg of peptide was dissolved in 500 µL of borate buffer (20 mM, pH 8.5) in the presence or absence of divalent cations at 1:1 M ratio with the peptide. The solution was sonicated for 1 min, vortexed three times for 5 s each, and transferred between the two plates of the rheometer. The geometry was lowered onto the sample to reach a gap of height between 0.8 and 1 mm, ensuring complete coverage of the plate and proper meniscus formation. The gelation test was performed at 25 °C. The time-dependent evolution of the storage (G′) and loss (G″) moduli was monitored by applying a constant dynamic strain of 1% at a constant frequency of 1 Hz every 10 min until a plateau was reached. Once the plateau was reached, a dynamic frequency sweep (frequency range: 0.1–10 Hz, at 1% strain) was conducted, followed by a temperature sweep test. For the temperature sweep, the temperature was progressively increased from 25 °C to 95 °C in 10 °C increments, and the degradation of the hydrogel was monitored by measuring the storage and loss moduli at a constant dynamic strain of 1% and a constant frequency of 1 Hz.

# Results and discussion

## Self-assembly of heterochiral peptide: effects of divalent cations into gelation

The objective of this study is to investigate the effects of four divalent cations ($Ca^{2+}$, $Mg^{2+}$, $Zn^{2+}$, and $Cu^{2+}$) on the structural, thermal, and mechanical properties of FINyVK- hydrogels.

Before assessing how divalent cations could modulate hydrogel formation, we determined the minimum gelation concentration (MGC) of the peptide alone using the tube inversion method (Maria Alonso et al., 2021). As shown in the upper panel of Figure 2, partial gelation was observed at 1 mM (Figure 2C), becoming complete at concentrations of 2 mM and above (Figures 2A,B).

Based on this analysis, we prepared hydrogel at 2 mM of peptide to observe the same condition in the presence of divalent cations, using a 1:1 M ratio of peptide to cation. As shown in the lower panel of Figure 2, in the presence of $Mg^{2+}$ and $Ca^{2+}$, self-supporting 3D hydrogels were formed (Figures 2H,I). Whereas in the presence of $Zn^{2+}$ and $Cu^{2+}$, only partial, non-self-supporting gelation was observed (Figures 2F,G).

This behavior can be better understood by examining both the coordination chemistry of the cations and the specific nature of the peptide sequence FINyVK.

As alkaline earth metals, $Ca^{2+}$ and $Mg^{2+}$, typically establish non-specific, labile interactions with charged or polar groups, including the amide side chain of asparagine (N) or the ε-amino group of lysine (K) (Ohki et al., 1997; Vasquez-Montes et al., 2022). These interactions can reinforce peptide-peptide associations while not interfering with the self-assembly process. Their coordination often promotes the creation of extensive hydrogen-bonding networks and hydrophobic clustering (e.g., involving F, I, and V), which enhances hydrogelation (Shao et al., 2020; Pal and Roy, 2022). Conversely, $Zn^{2+}$ and $Cu^{2+}$, as transition metals, demonstrate more robust and specific coordination characteristics. They exhibit a strong attraction to nitrogen and oxygen donors, specifically aiming at side chains such as those found in asparagine and lysine (Rulíšek and Vondrášek, 1998; Myari et al., 2001). Moreover, they could engage with the phenolic hydroxyl group of D-tyr, possibly changing its alignment or affecting nearby arrangements (Remko et al., 2011; Bhunia et al., 2017). These tighter and more directional interactions might disrupt the fragile equilibrium of non-covalent forces as

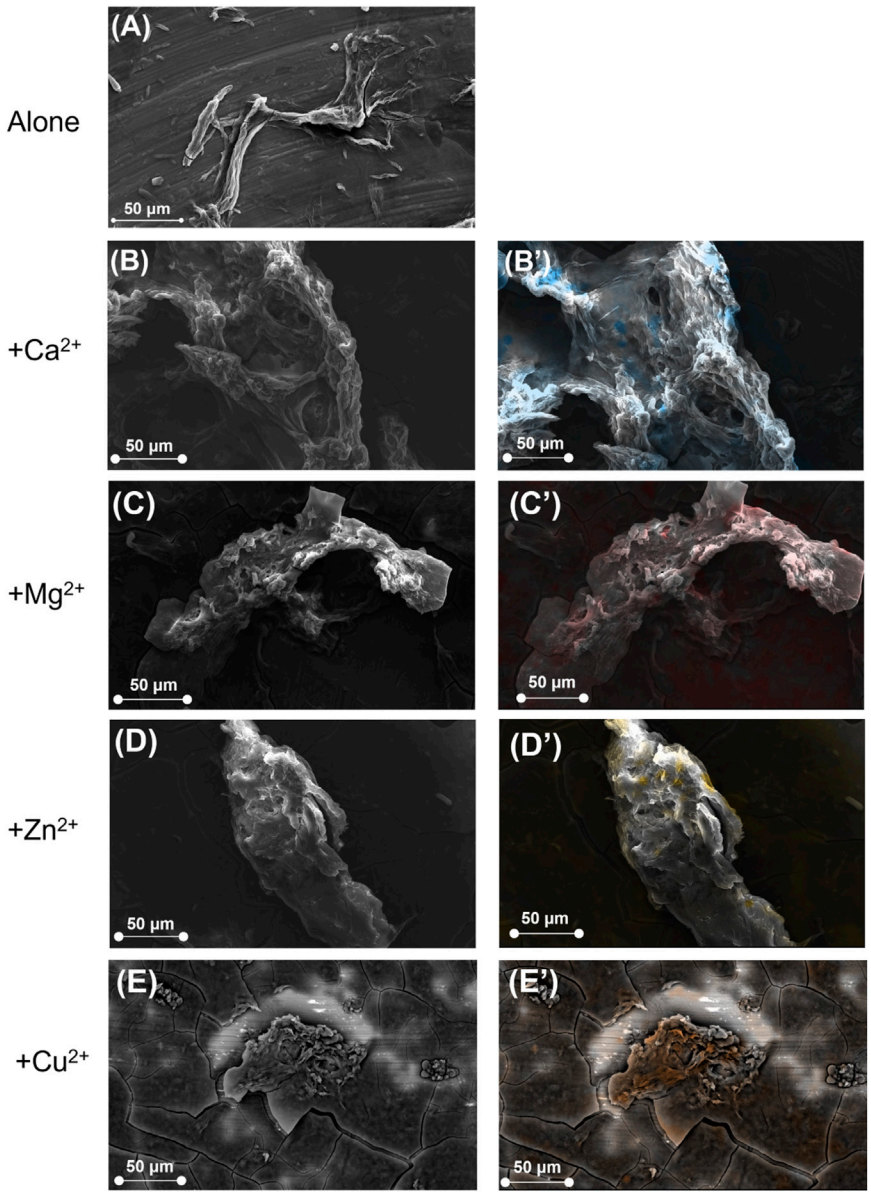


FIGURE 3
SEM images of the hydrogels obtained from FINyVK peptide alone **(A)** and in the presence of bivalent metal cations **(B)** $Ca^{2+}$, **(C)** $Mg^{2+}$, **(D)** $Zn^{2+}$, **(E)** $Cu^{2+}$. The right column **(B′–E′)** reports the corresponding EDS mapping performed in live mode using ChemiSEM technology. Metal ions are indicated by the following colors: blue for $Ca^{2+}$, red for $Mg^{2+}$, yellow for $Zn^{2+}$ and orange for $Cu^{2+}$.

hydrophobic, π–π stacking (e.g., involving F and y), and hydrogen bonding, that facilitate gel formation (Ruan and Rodgers, 2004; Sharma et al., 2019).

## Morphological analysis

SEM analysis with EDS mapping was performed to gain insights into the morphology of supramolecular structures (Figure 3). The peptide exhibited a tightly packed fibrous network, with an average fiber mesh thickness of 0.55 ± 0.06 µm and small pores measuring approximately 0.7 ± 0.1 µm (Table 1). In the presence of $Ca^{2+}$, both parameters showed a notable increase, resulting in a thicker and more porous network structure, with mesh thickness measuring 2.9 ± 0.5 µm and pore width 3.6 ± 0.6 µm $Zn^{2+}$ also facilitated the formation of thicker meshes (2.4 ± 0.4 µm) and broader pores (2.1 ± 0.5 µm), albeit to a reduced degree compared to calcium. In comparison, the inclusion of $Mg^{2+}$ resulted only in a slight increase in fiber thickness (0.70 ± 0.09 µm) with respect to FINyVK alone, and no distinctly defined pores were seen. $Cu^{2+}$ resulted in a moderate effect, indicating a partially organized network.

The SEM analysis is consistent with the macroscopic observations of hydrogels. Indeed, the presence of $Ca^{2+}$ and $Mg^{2+}$ resulted in networks with thicker fibrils and notably larger pores in the case of $Ca^{2+}$, compared to the pure FINyVK-based hydrogel

TABLE 1 Average fiber mesh thickness and average pore width of the indicated hydrogels, as measured from SEM micrographs (Supplementary Figure S1).

| Samples | Average fiber mesh thickness (μm) | Average pore width* (μm) |
|---|---|---|
| FINyVK | 0.55 ± 0.06 | 0.7 ± 0.1 |
| FINyVK + $Ca^{2+}$ | 2.9 ± 0.5 | 3.6 ± 0.6 |
| FINyVK + $Mg^{2+}$ | 0.70 ± 0.09 | No pores are present |
| FINyVK + $Zn^{2+}$ | 2.4 ± 0.4 | 2.1 ± 0.5 |
| FINyVK + $Cu^{2+}$ | 1.3 ± 0.3 | 1.0 ± 0.2 |

*Distance between fiber meshes.

(Table 1). Consistently, the observed self-supporting gels appeared macroscopically compact at visual detection (Figures 2H,I). In contrast, the rise in fiber thickness for $Zn^{2+}$ and $Cu^{2+}$ embedding hydrogels is associated with reduced homogeneity and decreased porosity (notably with $Cu^{2+}$). This morphological arrangement corresponds with the observed partial and non-self-supporting gelation behavior (Figures 2F,G).

Energy Dispersive X-ray Spectroscopy (EDS) was integrated with SEM analysis to evaluate the spatial distribution of metal ions within the hydrogel network (Figures 3B'–E') (Newbury and Ritchie, 2014). The EDS mapping revealed a generally homogeneous distribution of cations within the hydrogel network, indicating effective incorporation during the gelation process.

## Conformational analysis

CD spectra of monomeric FINyVK in the absence and in the presence of divalent cations were recorded during time to gain a deeper understanding of the self-assembly mechanism of the heterochiral peptide (Supplementary Figure S2). The peptide alone exhibited two minima centered at 204 and 227 nm which resulted not affected by the presence of divalent cations and during time.

Analogously, the influence of selected cations in tuning final hydrogel structure and thermal stability was estimated (Figure 4).

In the case of FINyVK alone (Figure 4A), an unexpected increase in the magnitude of the CD signal at 220.6 nm was observed upon heating up to 65 °C. Subsequently, the signal gradually decreased as the temperature approached 90 °C, returning to a value comparable to that recorded at the initial 20 °C. The overlay of CD spectra revealed a slight shift of the minimum from 220.6 nm (at 20 °C) to 222.6 nm (at 60 °C). A possible explanation consists in the fact that hydrogels often swell or shrink with temperature changes, affecting hydration (Liu et al., 2019; Chung et al., 2021). Dehydration and/or phase transition can reduce dielectric screening and lead to better alignment or packing, thereby enhancing CD response (Nicolini et al., 2004; Lignell et al., 2009). At moderate temperature increases, enhanced mobility can help molecules to explore more favorable conformations or pack more tightly.

The peptide hydrogel alone thus demonstrated moderate stability since the CD spectra at 20 °C, 90 °C and after returning to 20 °C (Supplementary Figure S3A) were nearly superimposable. In contrast, when the sample, after being cooled to 20 C, was abruptly reheated to 90 °C, in a discontinuous way, a clear reduction of CD signal is observed likely due to the partial disruption of ordered structures and the onset of aggregation (Supplementary Figure S3B) (Denisov and Halle, 1998; Manderson et al., 1999; Benjwal et al., 2006). Nevertheless, this change was reversible: upon cooling back to 20 °C, the CD spectrum closely resembled the original spectrum recorded at 20 °C.

In the case of FINyVK + $Ca^{2+}$ (Figure 4B), a reduction of CD signal and a concomitate shift of the wavelength of the minimum was observed (from 224 nm to 227 nm) during temperature increase, with a partial loss of ordered conformations. In this case, the re-cooling of the sample at 20 °C produced a CD spectrum not superimposable to the initial at 20 °C but more like that at 90 °C suggesting no reversibility of the partial denaturation (Supplementary Figure S3C). However, the not continuous heating at 90 °C did not provide further denaturation (Supplementary Figure S3D). Conversely, the presence of $Mg^{2+}$ determined the absence of a significant variation of CD signal, Figure 4C, and no shift of the minimum, suggesting a stabilizing effect of this cation greater to that observed for $Ca^{2+}$. In this case, the re-heating at 90 °C, in a discontinuous manner, determined a slight reduction of the Cotton effect which was maintained also in the re-cooling at 20 °C (Supplementary Figure S3F). Effects similar to $Mg^{2+}$ were caused by the presence of $Cu^{2+}$ ion: indeed, the CD signal did not significantly change upon temperature increase Figure 4D, as well as no changes of minimum was observed. However, the re-heating of the sample to 90 °C (Supplementary Figure S3H) determined a shift of the minimum at 233 nm and a reduction of CD signal similar to that observed for FINyVK peptide alone (Supplementary Figure S3B). The addition of $Zn^{2+}$ ion determined a classical denaturation profile of the CD signal upon temperature increase, Figure 4E, but this denaturation was not reversible as (Supplementary Figures S3I,J) since CD spectra at 20 °C, before and after heating, were not superimposable.

## Rheological studies

For the gelation studies, FINyVK solutions prepared in the absence and presence of selected divalent cations were loaded between the parallel plates of the rheometer. The gelation profiles, reported in Figure 5A, demonstrated that, after 10 min, gel formation is substantially initiated for all tested formulations, as indicated by a storage modulus (G′) markedly higher than the loss modulus (G″) (Anderson et al., 2009). This feature suggests a significant transition from a liquid-to a solid-like state within this time. However, differences among the hydrogels were evident from the gelation test: the hydrogel formed of the peptide alone exhibited

10.3389/fddsv.2025.1673051

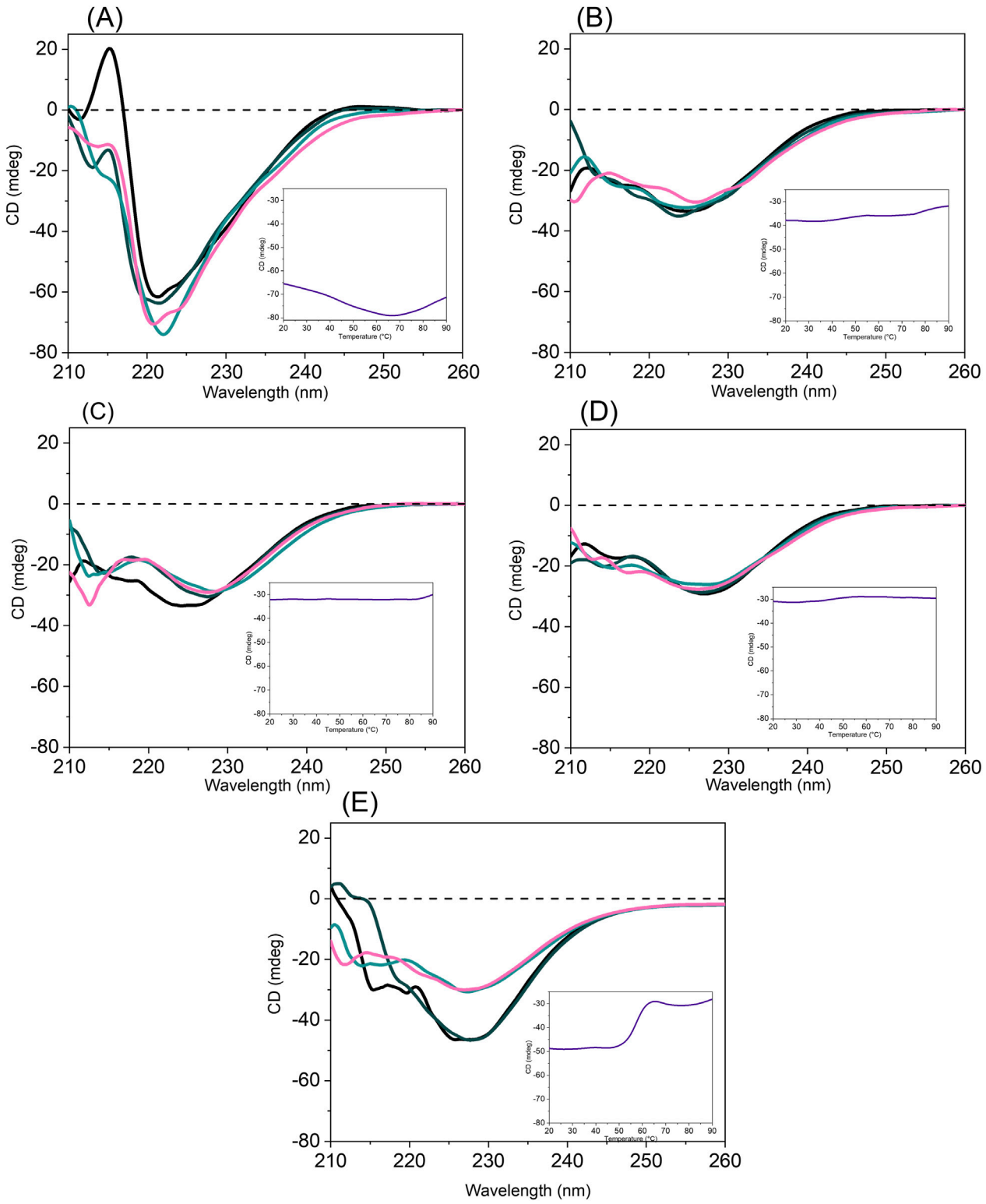


FIGURE 4
Overlay of the spectra collected at 20 (black), 40 (dark cyan), 60 (light cyan), 80 °C (magenta) for **(A)** FINyVK alone, **(B)** FINyVK + $Ca^{2+}$, **(C)** FINyVK + $Mg^{2+}$, **(D)** FINyVK + $Cu^{2+}$, **(E)** FINyVK + $Zn^{2+}$. Temperature profiles of the CD signal at the minimum wavelength are reported as insets (purple lines).

the slowest gelation kinetic, although the tan δ value (G″/G′) remained essentially unchanged throughout the process, indicating stable viscoelastic network development (Yucel et al., 2008). The presence of divalent cations generally accelerated the gelation process, with the exception of $Cu^{2+}$, which did not significantly enhance the kinetic compared to the peptide alone.

10.3389/fddsv.2025.1673051

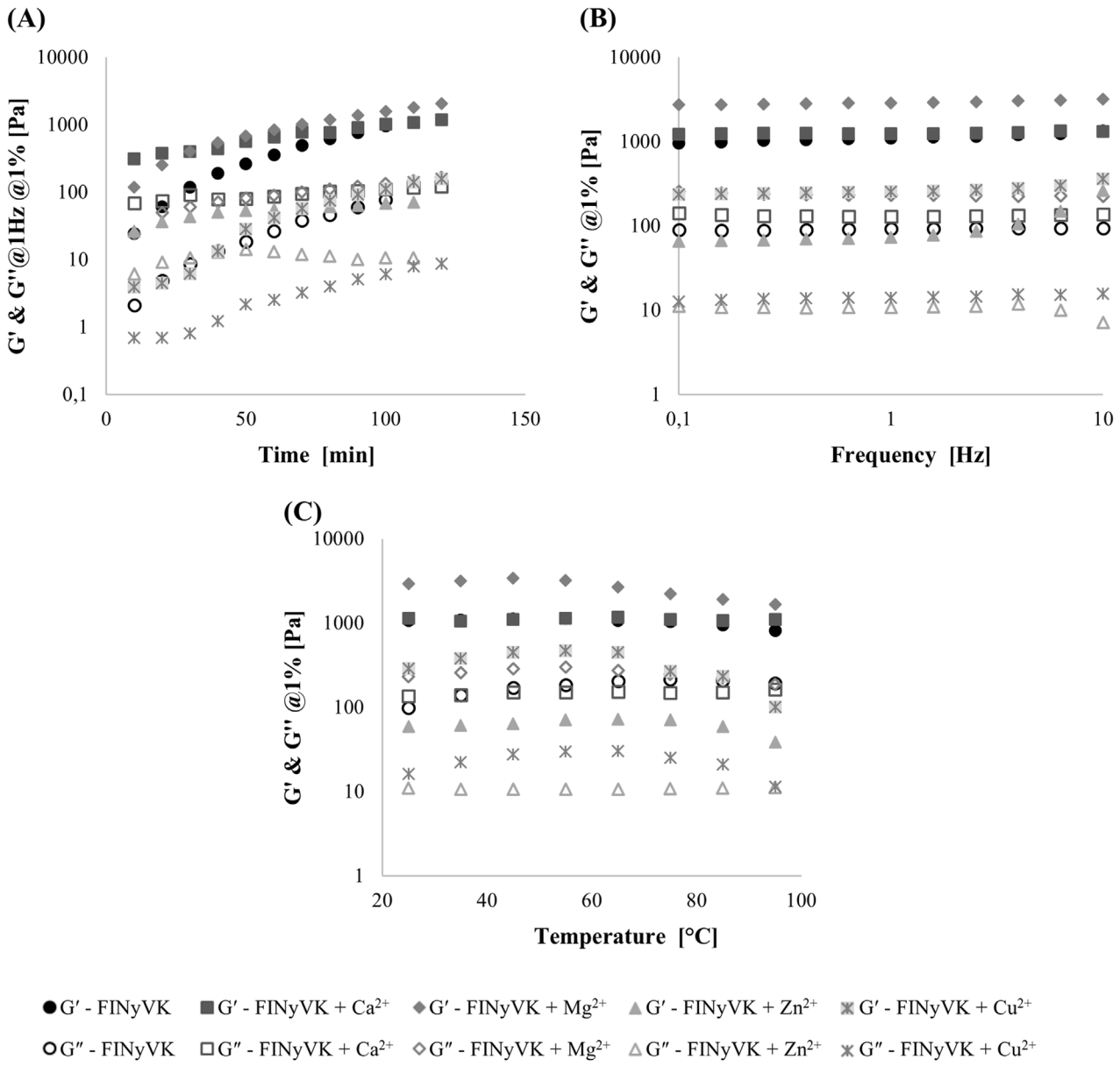


FIGURE 5
Hydrogel rheological characterization for FINyVK: alone (circle symbols), + $Ca^{2+}$ (square symbols), + $Mg^{2+}$ (rhombus symbols), + $Zn^{2+}$ (triangle symbols), and + $Cu^{2+}$ (asterisk symbols). Storage modulus (*G′*, solid symbols) and loss modulus (*G″*, open symbols) in gelation test **(A)**, frequency sweep **(B)**, and temperature sweep **(C)**.

Frequency sweep experiments were conducted at 1% strain over a frequency range from 0.1 to 10 Hz (Figure 5B). All hydrogels exhibited frequency-independent behavior, with tan δ values (G″/G′) lower than or close to 0.1, indicating a strong gel-like character (Table 2). The only exception was the hydrogel formed in the presence of $Zn^{2+}$, for which tan δ values ranged between 0.2 and 0.1 up to 4 Hz, suggesting a medium-strength gel behavior (Table 2). In addition, the presence of $Mg^{2+}$ led to an approximately threefold increase in the storage modulus (G′), whereas $Ca^{2+}$ induced only a marginal increase in G′ at low frequencies. In contrast, $Cu^{2+}$- and especially $Zn^{2+}$- caused a significant decrease in the viscoelastic

TABLE 2 Storage moduli (*G′*), loss modulus (*G″*) and tan δ (G″/G′) extracted from the frequency sweeps at 1 Hz for the hydrogels analyzed in this study.

| Samples | G′ (Pa) | G″ (Pa) | G″/G′ (Pa) |
|---|---|---|---|
| FINyVK | 1,110 | 93 | 0.08 |
| FINyVK + $Ca^{2+}$ | 1,240 | 129 | 0.1 |
| FINyVK + $Mg^{2+}$ | 2,900 | 230 | 0.08 |
| FINyVK + $Zn^{2+}$ | 74 | 11 | 0.15 |
| FINyVK + $Cu^{2+}$ | 255 | 14 | 0.06 |

moduli, which is consistent with the morphological data describing the formation of a gel with reduced homogeneity and partial, non-self-supporting gelation behavior. Finally, a thermal stability test was performed by increasing the temperature from 25 °C to 95 °C at a rate of 10 °C/min. The results, shown in Figure 5C, indicated that all hydrogels remained substantially stable up to approximately 65 °C, with a partial decline in their mechanical properties observed starting at 75 °C for the gels formed in the presence of $Cu^{2+}$ and $Mg^{2+}$. In contrast, the hydrogel formed in the presence of $Ca^{2+}$ maintained its stability up to 95 °C.

## Conclusion

Hydrogels have rapidly advanced in recent years due to their broad potential in biomedical applications and smart devices. Ensuring high performance is critical for their applications. One effective strategy for improving their properties is to incorporate divalent metal ions. In this study, we demonstrated that the self-assembly behaviour and hydrogel features of the ultrashort heterochiral peptide FINyVK can be effectively modulated by coordinating with specific divalent metal cations. Specifically, the weak coordination established between $Ca^{2+}$ and $Mg^{2+}$ and the peptide sequence accelerates sol-gel transitions and reinforces the peptide-peptide interactions, resulting in ultimate hydrogels characterized by thicker and more spaced fibers, exhibiting reversible thermal-induced conformational modification. This framework with enhanced porosity facilitates the loading of guest therapeutics, offering a suitable platform for drug delivery. Conversely, the strong coordination peptide-to-metal established by $Cu^{2+}$ and especially $Zn^{2+}$ cations with D-tyr residue adversely affects the final hydrogel structure, and moreover, the presence of Phe, which can participate in cation–π interactions, further compromises the integrity of the hydrogel. However, given the intrinsic antimicrobial activity of $Zn^{2+}$ and $Cu^{2+}$ cations, a rational combination of cations with complementary structural and biological functions (e.g., $Mg^{2+}$ for gel integrity and $Cu^{2+}$ for antimicrobial action) could represent an innovative strategy for developing multifunctional bioinspired materials.

## Data availability statement

The original contributions presented in the study are included in the article/Supplementary Material, further inquiries can be directed to the corresponding author.

## Author contributions

GP: Formal Analysis, Investigation, Writing – review and editing. DF: Formal Analysis, Investigation, Writing – review and editing. LC: Formal Analysis, Investigation, Writing – review and editing. PAN: Writing – review and editing. VP: Investigation, Writing – review and editing. DM: Conceptualization, Writing – review and editing. SLM: Formal Analysis, Investigation, Supervision, Writing – original draft, Conceptualization.

## Funding

The author(s) declare that financial support was received for the research and/or publication of this article. This work was supported by #NEXTGENERATIONEU (NGEU), Ministry of University and Research (MUR), National Recovery and Resilience Plan (NRRP), project MNESYS (PE0000006) – A Multiscale integrated approach to the study of the nervous system in health and disease (DN. 1553 11.10.2022).

## Acknowledgments

DF and LC acknowledge Ministero della Salute "Ricerca Corrente" project L3N9: "*Aggregazione proteica e amiloidogenesi: mutazioni, malattie e nuove frontiere teranostiche*."

## Conflict of interest

The authors declare that the research was conducted in the absence of any commercial or financial relationships that could be construed as a potential conflict of interest.

## Generative AI statement

The author(s) declare that no Generative AI was used in the creation of this manuscript.

Any alternative text (alt text) provided alongside figures in this article has been generated by Frontiers with the support of artificial intelligence and reasonable efforts have been made to ensure accuracy, including review by the authors wherever possible. If you identify any issues, please contact us.

## Publisher's note



## Supplementary material

The Supplementary Material for this article can be found online at: https://www.frontiersin.org/articles/10.3389/fddsv.2025.1673051/full#supplementary-material

# References


Anderson, J. M., Andukuri, A., Lim, D. J., and Jun, H. W. (2009). Modulating the gelation properties of self-assembling peptide amphiphiles. *ACS Nano* 3, 3447–3454. doi:10.1021/nn900884n

Benjwal, S., Verma, S., Röhm, K.-H., and Gursky, O. (2006). Monitoring protein aggregation during thermal unfolding in circular dichroism experiments. *Protein Sci.* 15, 635–639. doi:10.1110/PS.051917406

Bhunia, S., Singh, A., and Ojha, A. K. (2017). Investigation of the encapsulation of metal cations (Cu2+, Zn2+, Ca2+ and Ba2+) by the dipeptide Phe–Phe using natural bond orbital theory and molecular dynamics simulation. *J. Mol. Model* 23, 88–12. doi:10.1007/s00894-017-3248-5

Chang, R., Yuan, C., Zhou, P., Xing, R., and Yan, X. (2024). Peptide self-assembly: from ordered to disordered. *Acc. Chem. Res.* 57, 289–301. doi:10.1021/acs.accounts.3c00592

Chen, B., Liang, Y., Zhang, J., Bai, L., Xu, M., Han, Q., et al. (2021). Synergistic enhancement of tendon-to-bone healing via anti-inflammatory and pro-differentiation effects caused by sustained release of Mg2+/curcumin from injectable self-healing hydrogels. *Theranostics* 11, 5911–5925. doi:10.7150/THNO.56266

Chen, H., Zhang, T., Tian, Y., You, L., Huang, Y., and Wang, S. (2022). Novel self-assembling peptide hydrogel with pH-tunable assembly microstructure, gel mechanics and the entrapment of curcumin. *Food Hydrocoll.* 124, 107338. doi:10.1016/J.FOODHYD.2021.107338

Chung, T., Han, I. K., Han, J., Ahn, K., and Kim, Y. S. (2021). Fast and large shrinking of thermoresponsive hydrogels with phase-separated structures. *Gels* 7, 18. doi:10.3390/GELS7010018

Clover, T. M., O'Neill, C. L., Appavu, R., Lokhande, G., Gaharwar, A. K., Posey, A. E., et al. (2020). Self-assembly of block heterochiral peptides into helical Tapes. *J. Am. Chem. Soc.* 142, 19809–19813. doi:10.1021/jacs.9b09755

De Soricellis, G., Fagnani, F., Colombo, A., Dragonetti, C., Roberto, D., Marinotto, D., et al. (2023). An attractive family of cyclometalated Ir(III) dyes functionalized with tryptophan for potential neuroimaging applications. *Dyes Pigments* 210, 111012. doi:10.1016/J.DYEPIG.2022.111012

Denisov, V. P., and Halle, B. (1998). Thermal denaturation of ribonuclease a characterized by water 17O and 2H magnetic relaxation dispersion. *Biochemistry* 37, 9595–9604. doi:10.1021/bi980442b

Fichman, G., and Gazit, E. (2014). Self-assembly of short peptides to form hydrogels: design of building blocks, physical properties and technological applications. *Acta Biomater.* 10, 1671–1682. doi:10.1016/J.ACTBIO.2013.08.013

Florio, D., Di Natale, C., Scognamiglio, P. L., Leone, M., La Manna, S., Di Somma, S., et al. (2021). Self-assembly of bio-inspired heterochiral peptides. *Bioorg Chem.* 114, 105047. doi:10.1016/J.BIOORG.2021.105047

Gao, F., Yang, X., and Song, W. (2024). Bioinspired supramolecular hydrogel from design to applications. *Small Methods* 8, 2300753. doi:10.1002/smtd.202300753

Gupta, S., Singh, I., Sharma, A. K., and Kumar, P. (2020). Ultrashort peptide self-assembly: front-runners to transport drug and gene cargos. *Front. Bioeng. Biotechnol.* 8, 504. doi:10.3389/fbioe.2020.00504

Hua, Y., and Shen, Y. (2024). Applications of self-assembled peptide hydrogels in anti-tumor therapy. *Nanoscale Adv.* 6, 2993–3008. doi:10.1039/D4NA00172A

Huang, W., Dong, H., Yan, Q., Deng, T., Li, X., Zhao, Z., et al. (2025). Disulfide-rich self-assembling peptides based on aromatic amino acid. *Small* 21, 2407464. doi:10.1002/smll.202407464

Kuila, S., and Nanda, J. (2024). Cysteine-based dynamic self-assembly and their importance in the origins of life. *ChemSystemsChem* 6, e202400022. doi:10.1002/SYST.202400022

La Manna, S., Di Natale, C., Onesto, V., and Marasco, D. (2021). Self-assembling peptides: from design to biomedical applications. *Int. J. Mol. Sci.* 22, 12662. doi:10.3390/IJMS222312662

La Manna, S., Florio, D., Di Natale, C., Lagreca, E., Sibillano, T., Giannini, C., et al. (2022a). Type C mutation of nucleophosmin 1 acute myeloid leukemia: consequences of intrinsic disorder. *Biochimica Biophysica Acta (BBA) - General Subj.* 1866, 130173. doi:10.1016/J.BBAGEN.2022.130173

La Manna, S., Florio, D., Panzetta, V., Roviello, V., Netti, P. A., Di, C., et al. (2022b). Hydrogelation tunability of bioinspired short peptides. *MarascoSoft Matter* 18, 8418. doi:10.1039/d2sm01385a

Levin, A., Hakala, T. A., Schnaider, L., Bernardes, G. J. L., Gazit, E., and Knowles, T. P. J. (2020). Biomimetic peptide self-assembly for functional materials. *Nat. Rev. Chem.* 4, 615–634. doi:10.1038/s41570-020-0215-y

Lignell, M., Tegler, L. T., and Becker, H. C. (2009). Hydrated and dehydrated tertiary interactions–opening and closing–of a four-helix bundle peptide. *Biophys. J.* 97, 572–580. doi:10.1016/J.BPJ.2009.04.055

Liu, C., Zhang, Q., Zhu, S., Liu, H., and Chen, J. (2019). Preparation and applications of peptide-based injectable hydrogels. *RSC Adv.* 9, 28299–28311. doi:10.1039/C9RA05934B

Manderson, G. A., Creamer, L. K., and Hardman, M. J. (1999). Effect of heat treatment on the circular dichroism spectra of bovine β-lactoglobulin A, B, and C. *J. Agric. Food Chem.* 47, 4557–4567. doi:10.1021/JF981291M

Marasco, D., Perretta, G., Sabatella, M., and Ruvo, M. (2008). Past and future perspectives of synthetic peptide libraries. *Curr. Protein Pept. Sci.* 9, 447–467. doi:10.2174/138920308785915209

Marasco, D., Simon, I., Florio, D., and Marasco, D. (2024). Could targeting NPM1c+ misfolding Be a promising strategy for combating acute myeloid leukemia? *Int. J. Mol. Sci.* 25, 811. doi:10.3390/IJMS25020811

Maria Alonso, J., Andrade del Olmo, J., Perez Gonzalez, R., Saez-Martinez Citation, V., del Olmo, A., Gonzalez, P., et al. (2021). Injectable hydrogels: from laboratory to industrialization. *Polymers* 13, 650. doi:10.3390/POLYM13040650

Melchionna, M., Styan, E., and Marchesan, S. (2016). The unexpected advantages of using D-amino acids for peptide self- assembly into nanostructured hydrogels for medicine. *Curr. Top. Med. Chem.* 16, 2009–2018. doi:10.2174/1568026616999160212120302

Mitrea, D. M., Cika, J. A., Stanley, C. B., Nourse, A., Onuchic, P. L., Banerjee, P. R., et al. (2018). Self-interaction of NPM1 modulates multiple mechanisms of liquid–liquid phase separation. *Nat. Commun.* 9, 842–13. doi:10.1038/s41467-018-03255-3

Mu, R., Zhu, D., Abdulmalik, S., Wijekoon, S., Wei, G., and Kumbar, S. G. (2024). Stimuli-responsive peptide assemblies: design, self-assembly, modulation, and biomedical applications. *Bioact. Mater* 35, 181–207. doi:10.1016/J.BIOACTMAT.2024.01.023

Myari, A., Malandrinos, G., Deligiannakis, Y., Plakatouras, J. C., Hadjiliadis, N., Nagy, Z., et al. (2001). Interaction of Cu2+ with His–Val–His and of Zn2+ with His–Val–Gly–Asp, two peptides surrounding metal ions in Cu,Zn-superoxide dismutase enzyme. *J. Inorg. Biochem.* 85, 253–261. doi:10.1016/S0162-0134(01)00204-5

Newbury, D. E., and Ritchie, N. W. M. (2014). Performing elemental microanalysis with high accuracy and high precision by scanning electron microscopy/silicon drift detector energy-dispersive X-ray spectrometry (SEM/SDD-EDS). *J. Mater Sci.* 50, 493–518. doi:10.1007/s10853-014-8685-2

Nicolini, C., Ravindra, R., Ludolph, B., and Winter, R. (2004). Characterization of the temperature- and pressure-induced inverse and reentrant transition of the minimum elastin-like polypeptide GVG(VPGVG) by DSC, PPC, CD, and FT-IR spectroscopy. *Biophys. J.* 86, 1385–1392. doi:10.1016/S0006-3495(04)74209-5

Ohki, S. Y., Ikura, M., and Zhang, M. (1997). Identification of Mg2+-binding sites and the role of Mg2+ on target recognition by calmodulin. *Biochemistry* 36, 4309–4316. doi:10.1021/bi962759m

Pal, V. K., and Roy, S. (2022). Cooperative metal ion coordination to the short self-assembling peptide promotes hydrogelation and cellular proliferation. *Macromol. Biosci.* 22, 2100462. doi:10.1002/mabi.202100462

Qian, J., Ji, L., Xu, W., Hou, G., Wang, J., Wang, Y., et al. (2022). Copper-hydrazide coordinated multifunctional hyaluronan hydrogels for infected wound healing. *ACS Appl. Mater Interfaces* 14, 16018–16031. doi:10.1021/acsami.2c01254

Remko, M., Fitz, D., Broer, R., and Rode, B. M. (2011). Effect of metal Ions ($Ni^{2+}$, $Cu^{2+}$ and $Zn^{2+}$) and water coordination on the structure of L-phenylalanine, L-tyrosine, L-tryptophan and their zwitterionic forms. *J. Mol. Model* 17, 3117–3128. doi:10.1007/s00894-011-1000-0

Ruan, C., and Rodgers, M. T. (2004). Cation-π interactions: structures and energetics of complexation of Na+ and K+ with the aromatic amino acids, phenylalanine, tyrosine, and tryptophan. *J. Am. Chem. Soc.* 126, 14600–14610. doi:10.1021/ja048297e

Rulíšek, L., and Vondrášek, J. (1998). Coordination geometries of selected transition metal ions (Co2+, Ni2+, Cu2+, Zn2+, Cd2+, and Hg2+) in metalloproteins. *J. Inorg. Biochem.* 71, 115–127. doi:10.1016/S0162-0134(98)10042-9

Russo, A., Diaferia, C., La Manna, S., Giannini, C., Sibillano, T., Accardo, A., et al. (2017). Insights into amyloid-like aggregation of H2 region of the C-terminal domain of nucleophosmin. *Biochimica Biophysica Acta (BBA) - Proteins Proteomics* 1865, 176–185. doi:10.1016/J.BBAPAP.2016.11.006

Sahu, I., and Chakraborty, P. (2024). A repertoire of nanoengineered short peptide-based hydrogels and their applications in biotechnology. *Colloids Surf. B Biointerfaces* 233, 113654. doi:10.1016/J.COLSURFB.2023.113654

Seidi, K., Ayoubi-Joshaghani, M. H., Azizi, M., Javaheri, T., Jaymand, M., Alizadeh, E., et al. (2021). Bioinspired hydrogels build a bridge from bench to bedside. *Nano Today* 39, 101157. doi:10.1016/J.NANTOD.2021.101157

Shao, T., Falcone, N., and Kraatz, H. B. (2020). Supramolecular peptide gels: influencing properties by metal ion coordination and their wide-ranging applications. *ACS Omega* 5, 1312–1317. doi:10.1021/acsomega.9b03939

Shao, T., Noroozifar, M., and Kraatz, H. B. (2024). Divalent metal ion modulation of a simple peptide-based hydrogel: self-assembly and viscoelastic properties. *Soft Matter* 20, 2720–2729. doi:10.1039/D3SM01544K

Sharma, P., Kaur, H., and Roy, S. (2019). Inducing differential self-assembling behavior in ultrashort peptide hydrogelators using simple metal salts. *Biomacromolecules* 20, 2610–2624. doi:10.1021/acs.biomac.9b00416

Shen, J., Dai, Y., Xia, F., and Zhang, X. (2022). Role of divalent metal ions in the function and application of hydrogels. *Prog. Polym. Sci.* 135, 101622. doi:10.1016/J.PROGPOLYMSCI.2022.101622

Tunn, I., Harrington, M. J., and Blank, K. G. (2019). Bioinspired Histidine¯Zn2+ coordination for tuning the mechanical properties of self-healing coiled coil cross-linked hydrogels. *Biomimetics* 4, 25. doi:10.3390/biomimetics4010025

Vasquez-Montes, V., Goldberg, A. F. X., Thévenin, D., and Ladokhin, A. S. (2022). Ca2+ and Mg2+ influence the thermodynamics of peptide-membrane interactions. *J. Mol. Biol.* 434, 167826. doi:10.1016/J.JMB.2022.167826

Wu, D., Cheng, S., Wu, C., Wang, L. S., El-Seedi, H., Zhao, G., et al. (2024). Zn2+-coordination-driven helical dodecapeptide assembly hydrogel. *Food Biosci.* 62, 105325. doi:10.1016/J.FBIO.2024.105325

Yu, T., Hu, Y., He, W., Xu, Y., Zhan, A., Chen, K., et al. (2023). An injectable and self-healing hydrogel with dual physical crosslinking for *in-situ* bone formation. *Mater Today Bio* 19, 100558. doi:10.1016/J.MTBIO.2023.100558

Yucel, T., Micklitsch, C. M., Schneider, J. P., and Pochan, D. J. (2008). Direct observation of early-time hydrogelation in β-hairpin peptide self-assembly. *Macromolecules* 41, 5763–5772. doi:10.1021/MA702840Q

Zhou, Y., Li, Q., Wu, Y., Li, X., Zhou, Y., Wang, Z., et al. (2023). Molecularly stimuli-responsive self-assembled peptide nanoparticles for targeted imaging and therapy. *ACS Nano* 17, 8004–8025. doi:10.1021/acsnano.3c01452